ORIGINAL PAPER

In vivo imaging of early stage apoptosis by measuring real-time caspase-3/7 activation

**Matteo Scabini · Fabio Stellari · Paolo Cappella ·
Sara Rizzitano · Gemma Texido · Enrico Pesenti**

Abstract In vivo imaging of apoptosis in a preclinical setting in anticancer drug development could provide remarkable advantages in terms of translational medicine. So far, several imaging technologies with different probes have been used to achieve this goal. Here we describe a bioluminescence imaging approach that uses a new formulation of Z-DEVD-aminoluciferin, a caspase 3/7 substrate, to monitor in vivo apoptosis in tumor cells engineered to express luciferase. Upon apoptosis induction, Z-DEVD-aminoluciferin is cleaved by caspase 3/7 releasing aminoluciferin that is now free to react with luciferase generating measurable light. Thus, the activation of caspase 3/7 can be measured by quantifying the bioluminescent signal. Using this approach, we have been able to monitor caspase-3 activation and subsequent apoptosis induction after camptothecin and temozolomide treatment on xenograft mouse models of colon cancer and glioblastoma, respectively. Treated mice showed more than 2-fold induction of Z-DEVD-aminoluciferin luminescent signal when compared to the untreated group. Combining D-luciferin that measures the total tumor burden, with Z-DEVD-aminoluciferin that assesses apoptosis induction via caspase activation, we confirmed that it is possible to follow non-invasively tumor growth inhibition and induction of apoptosis after treatment in the same animal over time. Moreover, here we have proved that following early apoptosis induction by caspase 3 activation is a good biomarker that accurately predicts tumor growth inhibition by anti-cancer drugs in engineered colon cancer and glioblastoma cell lines and in their respective mouse xenograft models.

Keywords Apoptosis · Z-DEVD-aminoluciferin · Caspase-3 · Bioluminescence imaging · Xenogen

Matteo Scabini and Fabio Stellari equally contributed to this paper.

M. Scabini · F. Stellari · S. Rizzitano · G. Texido · E. Pesenti
Pharmacology Department, Oncology, Nerviano Medical
Sciences, Viale Pasteur 10, 20014 Nerviano, Italy

P. Cappella (✉)
Biology Department, Oncology, Nerviano Medical Sciences,
Viale Pasteur 10, 20014 Nerviano, Italy
e-mail: paolo.cappella@nervianoms.com

Introduction

Bioluminescence imaging (BLI) is a powerful methodology that has been developed over the last decade as a tool for the understanding of biological processes as they occur in living organisms. Recently, this non-invasive technology has evolved into a potentially more valuable aid for assessing cellular and molecular features of biology and disease in real time.

Apoptosis, or programmed cell death, is a highly regulated process essential for life of multi-cellular organisms. Its dysregulation plays a fundamental role in several diseases, including cancer [1]. In fact, one hallmark of human cancers resides in their ability to avoid apoptosis [2]. Thus, inducing apoptosis in tumor cells is an extremely promising approach as anti-cancer therapy. Indeed, many chemotherapeutic drugs exert their effects by inducing a final common pathway that leads to apoptosis. Agents that are widely used for cancer treatment, such as temozolomide (TMZ, guanine methylating agent) and camptothecin (CPT-11, topoisomerase-I inhibitor) cause DNA damage and finally induce apoptosis through a pathway that, although it has not been clearly understood, involves caspase 3 activation as the main player in tumor cell death induced by treatment with these agents [3, 4].

Caspases constitute a family of cysteine proteases that specifically contribute to the initiation and the execution of different steps in the apoptotic signaling cascade. To date, 14 caspases have been identified in humans and they can broadly be divided into initiator and effector caspases. Each caspase remains in an inactive procaspase form within the cell and it is only after the apoptotic induction stimuli that it becomes activated and cleaves its cellular substrates by binding to small specific peptide sequence [5].

Caspase-3 represents the central effector caspase in mammalian cells and is finally activated by either intrinsic or extrinsic apoptotic pathways [6]. The substrate-binding cleft of caspase-3 recognizes specifically a short 4-amino-acid stretch (DEVD) within protein substrates, directly N-terminal to the cleavage site [7]. This tetrapeptide motif is sufficient to bind specifically to the active caspase-3 and it is present in many cellular proteins (e.g., poly ADP ribose polymerase and lamins) [8]. As caspase-3 plays a vital role in mediating the initiation and the propagation of the apoptotic cascade, approaches that image its activation in a non-invasive way have been developed with the aim to provide a window of opportunity for the preclinical evaluation of therapeutics in animals in vivo over long time intervals.

Fluorochrome-labeled inhibitors of caspase (FLICA), which have been designed as affinity labels of the caspase active site, demonstrated their successful use in the detection of apoptosis activity within the in vitro and in vivo research setting [9]. However, additional findings have led to doubts as to the specificity of the staining by various fluorescent-labeled inhibitors of caspases, since the fluorescent signal was also originated from aspecific binding of FLICA [10]. Activatable probes with a quencher and an active fluorochrome separated by DEVD sequence could potentially provide readout for caspase activation in mouse tumor models. Nevertheless, as these probes are still under development [11], they cannot be applied in vivo yet.

Additional approaches that use fluorescence for the in vivo monitoring of apoptosis involve cells expressing a modified reporter proteins [12] linked to a DEVD tetrapeptide, which will emit light only after activation of caspase 3. However, strategies that rely on fluorescent signals have drawbacks when used in vivo because of the high scattering and the high auto fluorescence rates of visible and near-infrared light in tissues and blood, thus resulting in lower signal to noise ratio [13, 14]. BLI is not influenced by unspecific background signal, hence the use of bioluminescence is generally preferred over fluorescence for imaging of living organisms. Moreover, BLI allows displaying deeper tumor-emitted signals (less than 1 cm from skin, [15]) and, in addition, no photobleaching occurs for bioluminescent signals.

The use of a caspase-3-activated luciferase enzyme has proved to be a sensitive tool to monitor in vivo caspase-3 activation, but this approach is generally time consuming and requires another reporter gene to measure the tumor burden [16]. Therefore, several laboratories, including ours, have evaluated the feasibility of using the Z-DEVD-aminoluciferin substrate, which releases active aminoluciferin only after the DEVD peptide has been cleaved by caspase-3, to evaluate apoptosis induction [17, 18]. Here we have assessed apoptosis and tumor growth inhibition triggered by camptothecin and temozolomide in colon cancer and glioblastoma cell lines, respectively, and the mouse xenograft models derived from these cell lines.

For this, we have used D-Luciferin and a new formulation of Z-DEVD-aminoluciferin for the assessment of tumor burden and apoptosis in the same luciferase-expressing animal (Fig. 1), permitting accurate data normalization. Moreover, we have validated BLI in vitro by western blot and by flow cytometry.

Our results support previous data from similar studies, which used different therapeutics and different tumor models as the ones evaluated here, and have demonstrated once more that monitoring the early apoptosis induction might serve as a suitable biomarker for the prediction of anti-cancer drug efficacy with respect to tumor mass reduction [18, 19].

Methods

Reagents and antibodies

Z-DEVD-aminoluciferin soluble substrate (VivoGlo™ Caspase-3/7 Substrate, Promega Corp.) was kindly provided by A. Bosetti (Promega Italia). D-Luciferin was purchased from Promega Corp. CPT-11 (Irinotecan),
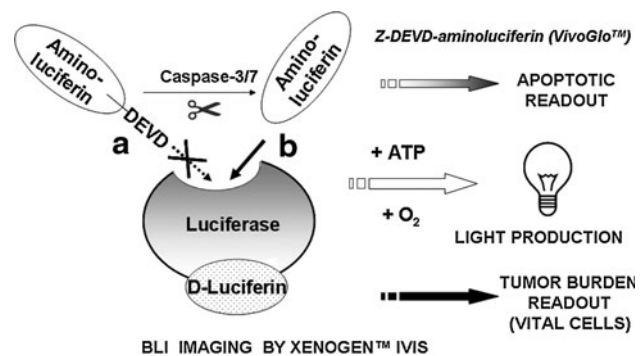
Fig. 1 Principle of bioluminescence quantification for apoptosis induction by a Caspase 3/7 substrate in vivo. When Z-DEVD-aminoluciferin is still linked to DEVD peptide, it cannot interact with luciferase because of steric hindrance whereas, after caspase cleavage, the released aminoluciferin is used by luciferase, together with ATP and O_2 to induce light. Subsequently, tumor burden is analyzed by D-Luciferin

temozolomide (TMZ) and ZVAD-FMK were obtained from Aventis, Sequoia Research Product Ltd and Zymed Laboratories Inc. (San Francisco, CA), respectively.

Anti-Tubulin gamma antibody was obtained from the Sigma-Aldrich Corporation. Anti-Caspase-3 (Asp 175) antibody was purchased from Cell Signaling Technology Inc. (Beverly, MA). Anti-PARP-1 antibody was purchased from Santa Cruz Biotechnology, Inc. (Santa Cruz, CA). Chemiluminescence western blot reagents were purchased from Amersham Pharmacia Biotech Inc. (Piscataway, NJ).

Cell lines and culture

The human colon cancer cell line HCT116 and the human glioblastoma cell line U251 were purchased from the American Type Culture Collection (ATCC, Manassas, VA).

HCT116 and U251 cell lines were transfected with pGL4.13 vector (Promega) using jetPEI (Polyplus) to create a stable luciferase expression clone selected by limited dilution (HCT116-Luc and U251-Luc, respectively).

HCT116-Luc and U251-Luc were maintained in McCoy's 5A and RPMI-1640 medium (Gibco BRL, Gaithersburg, MD), respectively, supplemented with 10% (v/v) heat-inactivated fetal bovine serum (Gibco BRL), 100 units/ml penicillin and 100 μg/ml streptomycin at 37°C in a humidified atmosphere containing 5% CO_2.

Western blot analysis

Cells were washed twice with PBS, scraped off from the dishes, and pelleted at 1000 g for 10 min. Cell pellets were then lysed in cold lysis buffer [2% SDS and 125 mM Tris–HCl (pH 7)].

Subcutaneous tumors were removed and immediately frozen in liquid nitrogen. 1 ml of cold lysis buffer (as described above) was added to 500 mg of frozen tissue, subsequently homogenized for 30 s and heated at 95°C for 15 min.

The lysates were clarified by centrifugation at 14,000 g for 15 min at 4°C. Identical amounts (50 μg of protein) of cell lysates were resolved in a 10% SDS-PAGE, and then proteins were transferred to a 0.45 μm nitrocellulose membranes. Membranes were incubated in blocking solution consisting of 5% powdered milk in TBST [10 mM Tris–HCl (pH 8), 150 mM NaCl, and 0.1% (v/v) Tween-20] for 1 h, then immunoblotted with the primary antibodies. Detection by enzyme-linked chemiluminescence was carried out according to manufacturer's protocol.

Flow cytometry

10^6 cells were fixed with 1% formaldehyde in PBS for 15 min at 37°C followed by dropwise methanol to 70% in

PBS and stored at 4°C. Cells were washed with PBS plus 1% FBS and permeabilized for 10 min with Triton X-100, 0.1% in PBS at 4°C.

After one wash with PBS, 1 μg per sample of rabbit anti-cleaved caspase-3 mAb in PBS was added and incubated for 1 h at room temperature. Thereafter, samples were washed with PBS solution and incubated with 0.5 μg per sample of AlexaFluor™ 488 conjugated goat anti-rabbit mAb for 1 h at room temperature. Cells were then washed with PBS before flow cytometry analysis. Cells were analyzed by dual laser 488/633 nm BD flow cytometry FACSCalibur™. DNA fragmentation was monitorered using red fluorescence log scale as already reported [20].

In vitro apoptosis detection using Z-DEVD-aminoluciferin substrate and ATP/luciferase quantification

10^5 HCT116-Luc and U251-Luc cells/well were plated in triplicate in a 96-well plate with 100 μl complete medium. 5 min before image acquisition 150 μg Z-DEVD-aminoluciferin were added to each well and BLI was detected using a charge coupled device camera in the IVIS imaging (Xenogen). 10^3 HCT116-Luc cells/well were plated in two 96-well plate with 100 μl complete medium. Cells were treated with SN-38 from 10 nM to 10 mM. 5 min before image acquisition 150 μg D-luciferin were added to each well. In the first plate, luciferase activity was monitored by Envision (PerkinElmer) luminometer. In the second plate, ATP was quantified using CellTiter-Glo assay (Promega) [21].

In vivo animal models

Male athymic nude mice (5 weeks old) obtained from Harlan Italy were housed in our barrier animal facility in sterile filter-top cages with 12-h light/dark cycles and fed with sterile rodent chow and water ad libitum. All animal studies were carried out in compliance with Italian Legislative Decree no. 116 dated January 27, 1992, and the European Communities Council Directive no. 86/609/EEC concerning the protection of animals used for experimental or other scientific purposes and according to institutional policy regarding the care and use of laboratory animals. HCT116-Luc and U251-Luc cell lines were inoculated subcutaneously (5 x 10^6 cells/mouse).

HCT116-Luc treated group ($n = 6$) received single 60 mg/kg CPT-11 i.v., while U251-Luc treated group ($n = 8$) received 50 mg/kg/day TMZ per os for 2 days. Mice were treated when subcutaneous tumors reached 100–200 mm^3.

Tumor growth was evaluated by both BLI and caliper measurements.
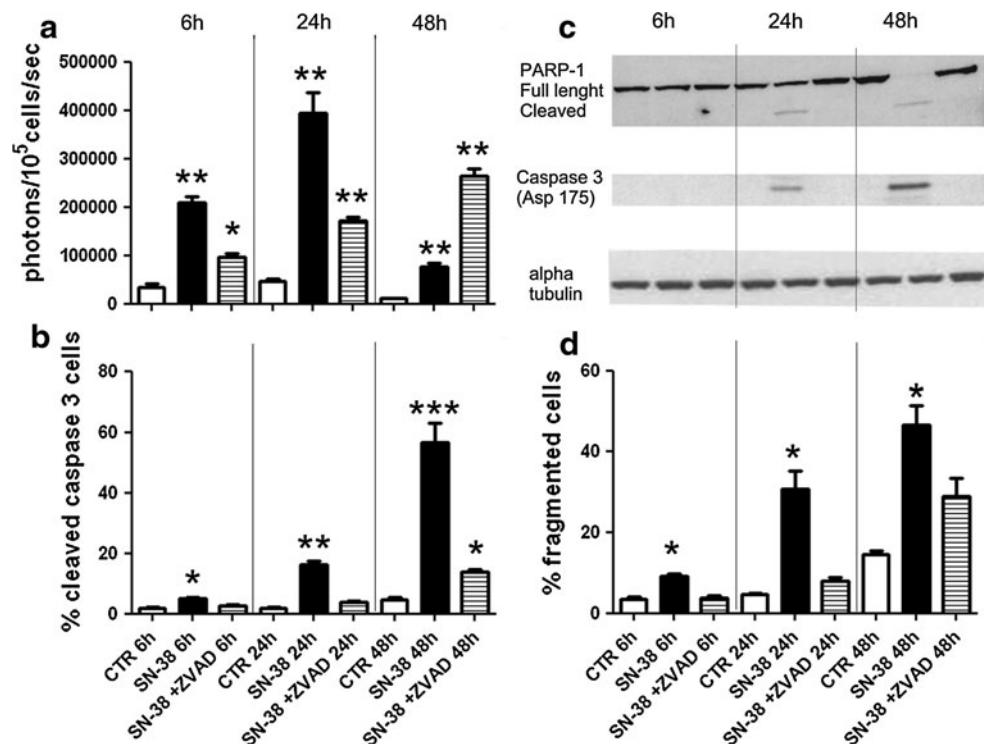
Bioluminescence Imaging

To monitor apoptosis induction, on established time-points after treatment, mice were injected i.p., with 50 mg/kg Z-DEVD-aminoluciferin in PBS, followed by anesthetization in 2–3% isoflurane atmosphere. From 10 to 60 min after injection of substrate, mice were imaged using a charge coupled device camera in the IVIS imaging. Signal intensity was quantified using a customized version of the IGOR Pro version 4.09A Software (WaveMetrics, Inc., Lake Oswego, OR) called Living Image version 3.00 (Xenogen). The sum of all detected photon counts from subcutaneous tumors was determined by evaluating automatically chosen ROI areas. Z-DEVD-aminoluciferin average signal from 10 to 60 min was calculated and normalized with D-luciferin signal. Briefly, 6 h after Z-DEVD-aminoluciferin injections (when no more bioluminescent signal could be detected) mice received 150 mg/kg D-luciferin i.p., followed by anesthetization in 2–3% isofluorane atmosphere. 10 min after the injection of substrate, mice were imaged as described above.

Statistical analysis

Results were analyzed for statistical significance using a Mann–Whitney t-test (Graph Pad Prism Software, San Diego, CA). P-value summary for each comparison with control was inserted in figures (*** $P < 0.001$; ** $0.001 < P < 0.01$; * $0.01 < P < 0.05$). P-value < 0.05 was considered statistically significant.

Results

BLI allows to measure apoptosis in vitro in cancer cells

To measure apoptosis directly in living cells, we first performed an optical imaging experiment in vitro by adding Z-DEVD-aminoluciferin to stably expressing luciferase cell lines (HCT116-Luc, U251-Luc) that had been treated with chemotherapeutics at different time-points. CPT-11 represents the gold standard treatment for human colon cancer whereas TMZ is at first line in glioblastoma treatment [22, 23]. As shown in Fig. 2a, treatment of HCT116-Luc cells with 1 μM SN-38, the active metabolite of CPT-11, enhanced the bioluminescent signal already at 6 h and reached its maximum at 24 h after treatment. Signal from control cells represented the basal level of apoptosis and remained constant through all the time-points. To test the specificity of Z-DEVD-aminoluciferin cleavage by caspase-3 and -7 we co-treated the cells with 40 μM ZVAD-FMK, a caspase-3 inhibitor [10]. ZVAD treatment reduced caspase-3 activation and subsequent cell death up to 24 h post-treatment time (Fig. 2a).

We performed a flow cytometry analysis using an anti-active-caspase-3 antibody to demonstrate that the luminescent signal from treated cells is really dependent on caspase-3 activation. In agreement with the Z-DEVD-aminoluciferin luminescent data, HCT116-Luc cells treated with SN-38 displayed an increase in active-caspase-3

Fig. 2 In vitro assay of caspase-3 activation in HCT116-Luc cells treated with SN-38. HCT116-Luc cells were treated with 1 μM SN-38 or co-treated with 40 μM ZVAD-FMK. Caspase-3 activation, 6, 24, and 48 h after treatment was measured by Z-DEVD-aminoluciferin BLI (a), by flow cytometry analysis using an antibody specific for active caspase-3 (b) and by Western blot analysis for the detection of active caspase-3 and PARP-1 cleavage (c). Percentage of cells with DNA fragmentation was measured by flow cytometry with propidium iodide (d). All the experiments were done in triplicate (error bars SD) and P-value summary was indicated for each group by asterisks

Fig. 3 Luciferase activity (**a**) and ATP quantification (**b**) in HCT116-Luc cells 6, 24, 48 and 72 h after SN-38 treatment and relative IC50 quantification by Graph Pad Prism. Luciferase activity decreased in a dose- and time-dependent manner and correlated with intracellular ATP concentration. As highlighted by *dotted line squares*, luciferase activity remained nearly unaffected at 6 and 24 h after 1 μM SN-38 treatment in conjunction with high level of intracellular ATP. Instead, as expected, 48 and 72 h after treatment lack of ATP caused luciferase activity decrease
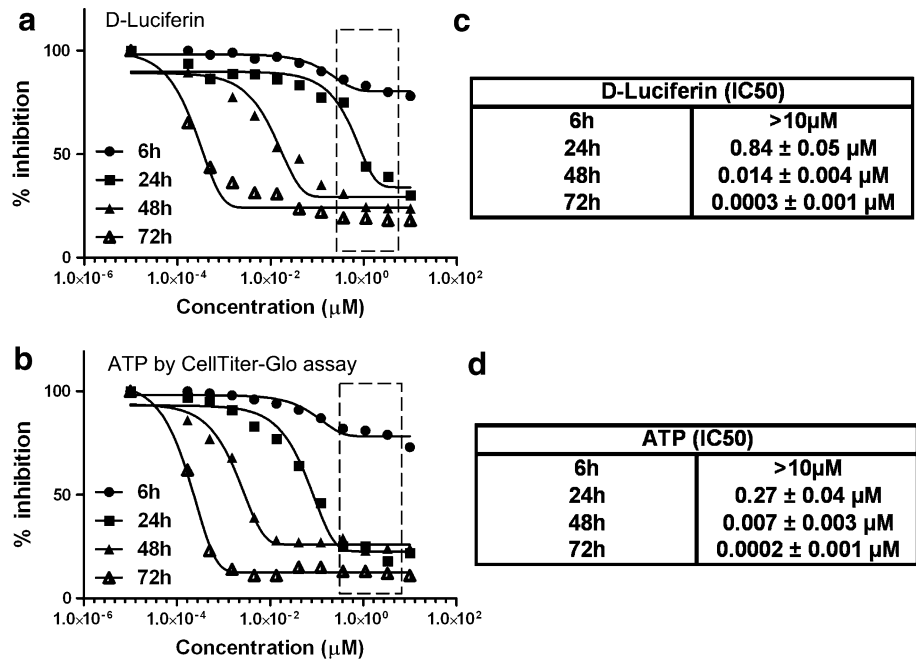
positive cells (Fig. 2b). Again, ZVAD-FMK co-treatment significantly blocked caspase-3 activation.

We also showed activation of caspase-3 by western blot analysis via PARP-1 cleavage, one of the main caspase-3 substrates (Fig. 2c). As already showed by flow cytometry analysis, ZVAD-FMK treatment reversed the SN-38 effect on caspase-3 activation. However, the incomplete caspase-3 inhibition upon ZVAD-FMK treatment suggests that Z-DEVD-aminoluciferin could be cleaved simultaneously by additional proteases.

A large amount of necrotic or late-apoptotic cells were present at 48 h after SN-38 treatment, as shown by DNA fragmentation analysis (Fig. 2d). Thus, cell death at 48 h after treatment was responsible for the Z-DEVD-amino-luciferin bioluminescent signal decrease that did not correlate with the percentage of active-caspase-3 positive cells measured by flow cytometry at this late time point. To support our hypothesis, dose response curves from 6 to 72 h after SN-38 treatment was performed to evaluate intracellular ATP concentration by CellTiter-Glo assay and D-Luciferin chemoluminescence induced by luciferase. As shown, lack of ATP during late apoptosis phases is responsible for the Z-DEVD-aminoluciferin biolumines-cent signal decrease (Fig. 3). Similarly, the treatment of U251-Luc cells with 2 mM TMZ resulted in a Z-DEVD-aminoluciferin bioluminescent signal increase while it remained constant in control cells and in cells co-treated with 40 μM ZVAD (Fig. 4a). These results were confirmed by flow cytometry analysis using active caspase-3 antibody demonstrating that, also for TMZ-treated U251-Luc cells, apoptosis is mediated by caspase-3 activation (Fig. 4b).

Caspase-3 activation and the subsequent PARP-1 cleavage in TMZ-treated cells, as compared with the control and ZVAD-FMK co-treatment, were showed also by western blot analysis (Fig. 4c). Again, DNA fragmentation, and subsequent cell death decreased Z-DEVD-aminolu-ciferin bioluminescent signal 48 h after TMZ treatment (Fig. 4d).

These results demonstrate that caspase-3 activation is required to induce apoptosis in HCT116-Luc and U251-Luc cell lines treated with chemotherapeutics and that the inhibition of caspase-3 blocks apoptosis progression and prevents cell death.

## BLI allows to measure apoptosis in vivo in xenograft models

In order to evaluate the feasibility of measuring apoptosis in vivo non-invasively, we extended this approach to HCT116-Luc and U251-Luc mouse xenograft models. Mice bearing subcutaneous HCT116-Luc tumors that had reached 100–200 mm^3 were treated with a single dose of CPT-11 at 60 mg/kg and were daily followed by BLI with both D-Luciferin and Z-DEVD-aminoluciferin. After 24 h, treatment with CPT-11 resulted in a 2,5-fold induction of Z-DEVD-aminoluciferin signal in the treated group when compared to the untreated one (Fig. 5a–d). As already shown in the in vitro experiments, the Z-DEVD-aminolu-ciferin signal from treated cells decreased at 48 h (Fig. 5e, f) and this was most likely due to cell death caused by chemotherapeutic drugs. The Z-DEVD-aminoluciferin signal was normalized with D-Luciferin to ensure that induction was not due to unspecific luciferase over-

Fig. 4 In vitro assay of caspase-3 activation on U251-Luc cells treated with TMZ. U251-Luc cells were treated with 2 mM TMZ or co-treated with 40 μM ZVAD-FMK. Caspase-3 activation, 6, 24 and 48 h after treatment was measured by Z-DEVD-aminoluciferin BLI (**a**), by flow cytometry analysis using active caspase-3 antibody (**b**) and by Western blot analysis following active caspase-3 and PARP-1 cleavage (**c**). Percentage of cells with DNA fragmentation was measured by flow cytometry with propidium iodide (**d**). All the experiments were done in triplicate (*error bars* SD) and *P*-value summary was indicated for each group by asterisks
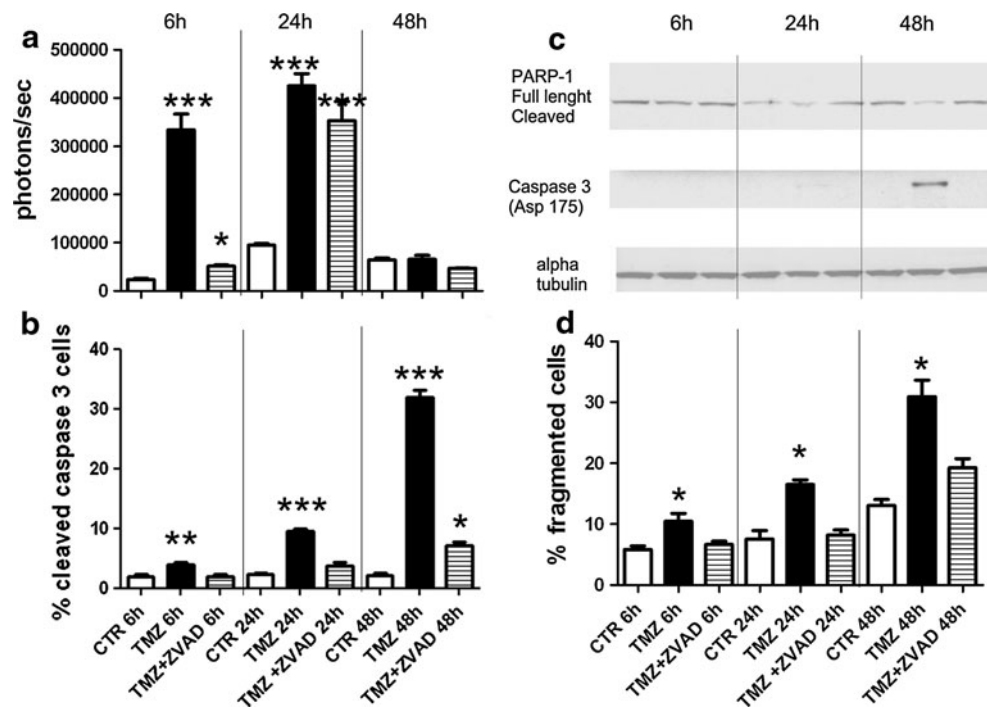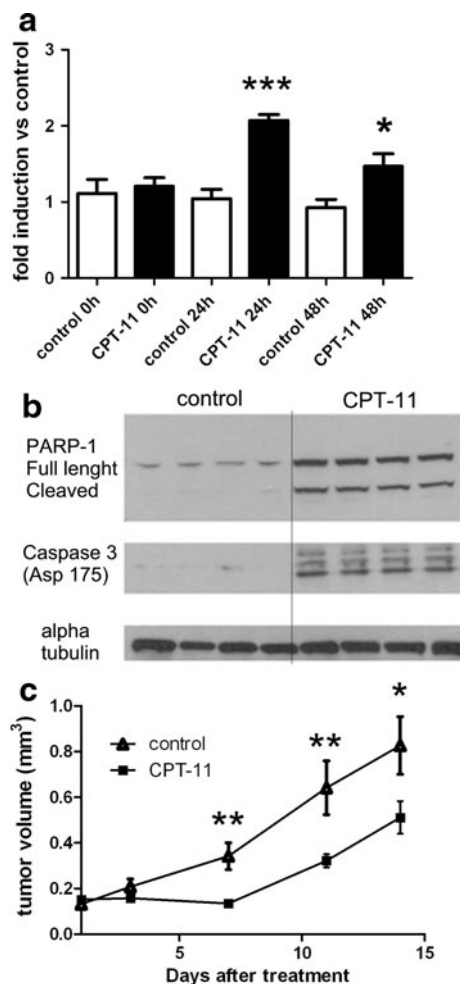

Fig. 5 Z-DEVD-aminoluciferin BLI on HCT116-Luc subcutaneous tumor model. HCT116-Luc xenograft mice were treated with a single dose of CPT-11 at 60 mg/kg. Mice (*n* = 6 per group) were injected i.p., with 50 mg/kg Z-DEVD-aminoluciferin in PBS (**a, c, e**) Bioluminescent signals were collected from 10 to 60 min after injection in untreated (*triangles*) or CPT-11 treated (*squares*) mice before (**a**) or 24 (**c**) and 48 (**e**) hours after treatment. (**b, d, f**) Representative images of Z-DEVD-aminoluciferin BLI at 40 min after Z-DEVD-aminoluciferin injection in untreated or CPT-11 treated mice before (**b**) or 24 (**d**) and 48 (**f**) hours after treatment. *Error bars* represent ± SEM and *P*-value summary was indicated for each group by asterisks
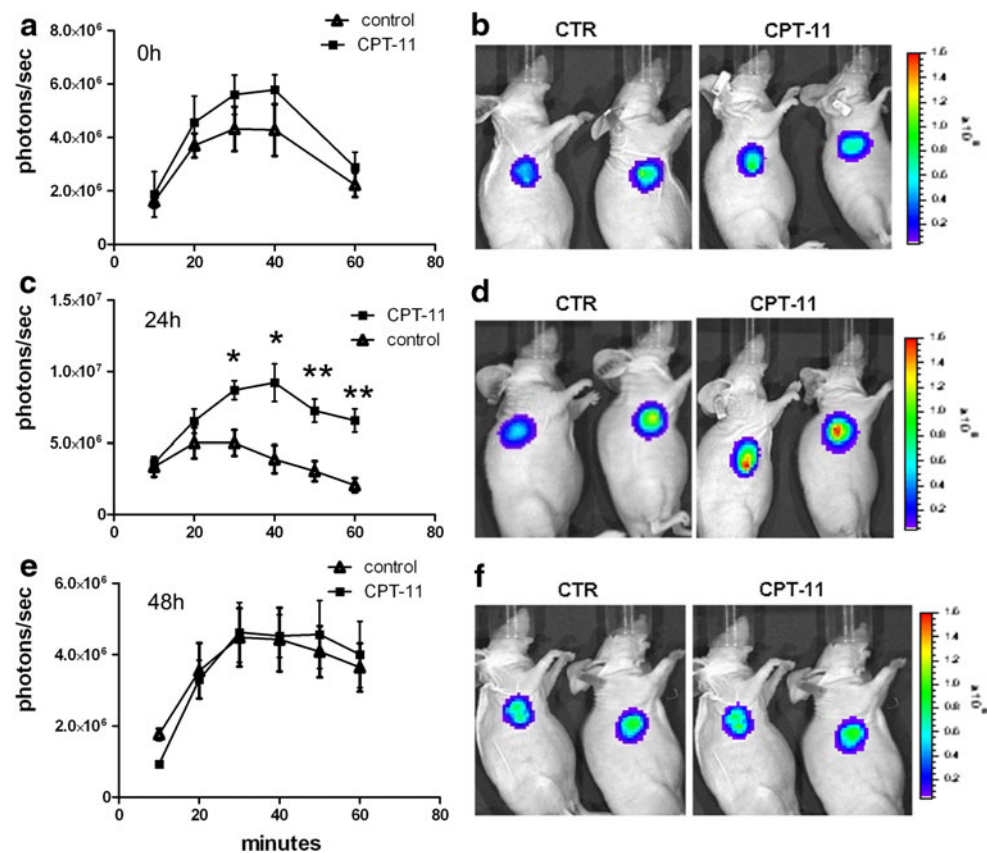
expression caused by the treatment (Fig. 6a). Ex vivo analysis by western blot demonstrated the activation of caspase-3 and subsequent PARP-1 cleavage at 24 h after

CPT-11 treatment (Fig. 6b). 1 week after treatment, caliper measurements demonstrated a significant tumor growth inhibition ($0.001 < P < 0.01$, 60% treated vs controls),
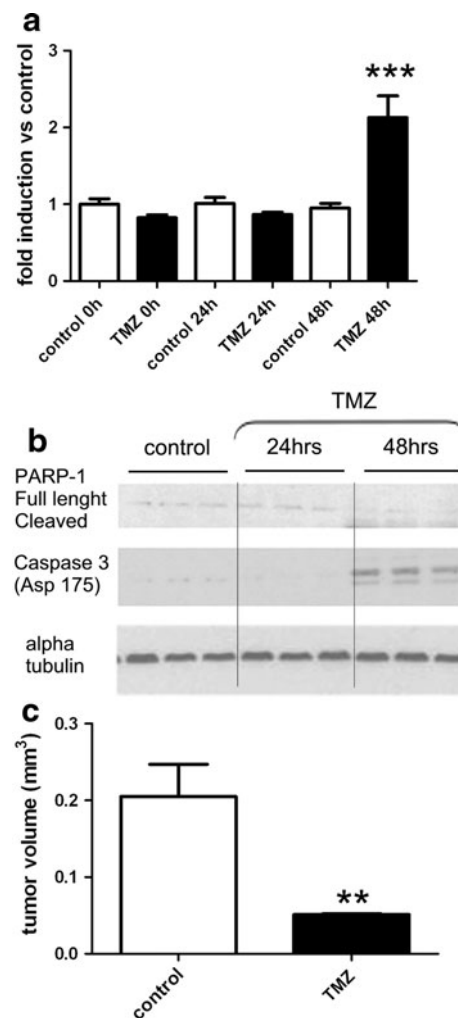
Fig. 6 In vivo measurement of apoptosis by Z-DEVD-aminoluciferin BLI in HCT116-Luc subcutaneous tumor model. (a) Caspase-3/7 activation on HCT116-Luc xenograft mice was followed by Z-DEVD-aminoluciferin BLI before or 24 and 48 h after a single dose of CPT-11 at 60 mg/kg. Z-DEVD-aminoluciferin luminescence signals were normalized with D-Luciferin signals both in untreated (*white bars*) and treated (*black bars*) animals ($n = 6$ *per* group). (b) Caspase-3 activation and PARP-1 cleavage at 24 h after treatment were demonstrated by ex vivo western blot analysis. Each *lane* represents the tumor lysate from one mouse. (c) HCT116-Luc subcutaneous tumor growth were followed by caliper measurements for 3 weeks after cells inoculation. CPT-11 treatment at day 8 showed tumor growth inhibition (*black squares*) compared to untreated tumor growth (*black triangles*). *Error bars* represent ± SEM and *P*-value summary was indicated for each group by asterisks

Fig. 7 In vivo measurement of apoptosis by Z-DEVD-aminoluciferin BLI in U251-Luc subcutaneous tumor model. **a** Caspase-3/7 activation on U251-Luc xenograft mice was followed by Z-DEVD-aminoluciferin BLI before or 24 and 48 h after the first 50 mg/kg TMZ treatment. Z-DEVD-aminoluciferin luminescence signals were normalized with D-Luciferin signals both in untreated (*white bars*) and treated (*black bars*) animals ($n = 8$ per group). **b** Caspase-3 activation and PARP-1 cleavage were demonstrated by ex vivo Western blot analysis. Each *lane* represents the tumor lysate from one mouse. **c** U251-Luc subcutaneous tumors showed a significant reduction 1 week after TMZ treatment (*black bar*) compared to untreated tumors (*white bar*). *Error bars* represent ± SEM and *P*-value summary was indicated for each group by asterisks

revealing that tumor cells died through apoptosis after a single CPT-11 injection (Fig. 6c).

Similarly, mice bearing 100–200 mm³ U251-Luc tumors were orally treated with 50 mg/kg/day TMZ for 2 days. TMZ induced 2-fold Z-DEVD-aminoluciferin signal increase in the treated group *versus* the control group 24 h after the second TMZ treatment (Fig. 7a).

Ex vivo analyses by western blot demonstrated TMZ-induced caspase-3 activation only 48 h after the first treatment (Fig. 7b), in agreement with in vitro western

blot analysis and with in vivo Z-DEVD-aminoluciferin results.

As observed in the HCT116-Luc xenograft model, 1 week after the two TMZ treatments, subcutaneous U251-Luc tumor burden was reduced by 70%, demonstrating that TMZ-treated tumor cells died upon apoptosis induction (Fig. 7c). In our experience, it was possible to monitor 4 days long the apoptosis in mice, without significant body weight loss or any other apparent sign of toxicity (data not shown).

Discussion

Since caspase family proteins are key mediators in the classical apoptosis pathway, detection of their proteolytic activity provides a useful assay for the analysis of early biochemical events associated with apoptosis in vivo.

Previous reports have already demonstrated that measuring caspase-3/7 activation using Z-DEVD-aminoluciferin in a bioluminescent assay is an extremely sensitive approach to measure apoptosis in vitro and also in vivo [17–19, 24]. However, the first preparation of Z-DEVD-aminoluciferin that was used in vivo appeared to be toxic and did not allow a second imaging session of the animal [17], and the new formulated Z-DEVD-aminoluciferin substrate that was utilized in most recent studies was not toxic but had solubility issues [18, 19]. In our study, we have used a new preparation of Z-DEVD-aminoluciferin that is not toxic and has an improved solubility. Actually, Z-DEVD-aminoluciferin could be dissolved in PBS because the improved solubility of this second generation preparation avoids the strong tendency toward peptide aggregation and precipitation at high concentrations [18, 19]. Utilizing this new preparation of Z-DEVD-aminoluciferin we have measured apoptosis both in vitro and in vivo in a sensitive and reproducible manner in two different cell lines, and their respective xenograft models, treated with apoptosis inducing chemotherapeutics. In vitro measurement of apoptosis using Z-DEVD-aminoluciferin has been validated by flow cytometry analysis, which detects signals at single cell level and, therefore, represents an accurate readout of cellular events. We have also shown that a single dose of CPT-11 at 60 mg/kg induces apoptosis in a colon cancer xenograft model and leads to tumor growth inhibition measured either by BLI and caliper 1 week after treatment. Similarly, TMZ induces apoptosis in a glioblastoma xenograft model 24 h after a 2-day treatment. Again in this case, 1 week after treatment we can observe tumor mass reduction. Apoptosis measured by BLI has been confirmed by ex vivo western blot analysis, which showed effective caspase-3 cleavage and its activation through the degradation of PARP-1, its specific substrate.

Normalization with D-Luciferin signal ensures that induction of Z-DEVD-aminoluciferin signal in treated mice is dependent on caspase-3 activation and it is not due to unspecific luciferase over-expression caused by the treatment. In fact, treatments that cause cell cycle inhibition have been observed to stimulate luciferase reporter vector to express more protein (data not shown). This leads to an artificial increase in bioluminescent signal that, however, can be normalized using D-Luciferin signal as reference. In this study, we have also demonstrated, for the first time, that the decrease in Z-DEVD-aminoluciferin

bioluminescent signal at late time points mainly depends on the decrease of intracellular ATP. Thus, cells in late stage apoptosis maintain activated caspase-3, as shown by flow cytometry analysis, but they are not viable anymore and, therefore, the lack of ATP does not allow the luciferase-luciferin reaction to continue. For this reason, paradoxically, Z-DEVD-aminoluciferin signal from treated cells at 48 h is lower than in the control ones and the correlation between BLI and percentage of cleaved caspase 3/7 cells is completely lost at the last time point (data not shown). This indicates that Z-DEVD-aminoluciferin bioluminescence represents the signal from vital and metabolically active cells that are already committed to die. However, the ATP quantification does not prove univocally the causal relation between light signal loss and the reduction of ATP levels, and it could be speculated that additional factors could contribute to this phenomenon.

It is known that cell death is associated with the breakdown of cancer tissues and the release of intra-cellular components; indeed, tumors are often associated with an acidic extra-cellular environment and the cytotoxic treatment of large volume tumors that are highly responsive to the treatment has been associated with the tumor lysis syndrome, culminating in acute renal failure and acidosis [25]. Moreover, in human leukaemia cells, it has been observed an increased lactate production following loss of mitochondrial membrane potential during apoptosis [26]. Firefly luciferase is very sensitive to pH variations, the pH decrease can lead to a reduced detectable light signals due to quantum yield reduction (quantum yield is 0.88 or 0.5, for pH 7.5 or 6.0 respectively), and pH dependent bathochromic (red) shifts occur due to the luciferase structure changes in an acidic environment. So far, lower pH values can adversely affect BLI, since the luciferase reaction emits less light at low pH [27].

Beyond the reduced levels of ATP and the decrease in pH, we cannot exclude that the loss of membrane integrity during the transition from apoptosis to necrosis, could lead to a reduction of additional cofactors that are required for light production in the luciferin-luciferase reaction.

The Z-DEVD-aminoluciferin signal increase observed in HCT116 cells treated with SN-38 and ZVAD-FMK 40 μM for 48 h might be explained by Z-DEVD-aminoluciferin cleavage by a protease other than caspase-3 [28, 29].

BLI is an ideal tool for high-throughput screening in preclinical setting. Firstly, BLI is relatively cost effective and user friendly. Furthermore, BLI is a non-invasive imaging technique and enables longitudinal monitoring of disease progression within the same animal. In this way, each animal can function as its own control, and this leads to a decreased amount of animals per study with a reduction in experimental costs. Finally, BLI produces images

that supply measurements of tumor growth that are neither subjective nor qualitative. Thus, BLI using Z-DEVD-aminoluciferin allows measuring, in vivo and in real-time, apoptosis induction after treatment at the desired timepoints without the need to sacrifice animals and to perform ex vivo analysis.

In our study we performed BLI measurement of apoptosis and total tumor burden in subcutaneous tumor models. However, BLI sensitivity combined with high tissue penetration of red-light emitted by luciferase (till 1 cm in depth) has allowed to extent the use of this method to other rodent tumor models and to models that develop tumors more internally in the organism, i.e., orthotopically implanted animal tumor models [15, 20].

So far, in clinical settings, many biomarkers have been validated for the evaluation of the activity of new compounds under development [30]. However, biomarker modulation and compound activity do not always reflect treatment efficacy in terms of tumor growth inhibition or disease regression [31]. Non-invasive measurement of apoptosis represents a new concept of biomarker which is a direct index of treatment efficacy in killing tumor cells.

In conclusion, in vivo imaging of apoptosis through Z-DEVD-aminoluciferin bioluminescence exploits imaging of vital cells to measure a death-committed signal. This paradoxical situation allows monitoring in vivo of both vital tumor cells and cells in early apoptosis, in the same animal and at the same time, without being affected by eventual necrosis areas that may be different from animal to animal. The sensitivity and accuracy offered by BLI open the door to a real-time PK/PD model through which to predict anti-tumor efficacy of newly developed compounds and, at the same time, to optimize their dose-scheduling. Moreover, as our studies are in agreement and support similar studies, even if they are based on different cancer models and have used different therapeutics, this emphasize the possibility to extend the use of this approach to a wide oncology research and to several development programs.

References

1. Hengartner MO (2000) The biochemistry of apoptosis. Nature 407:770–776
2. Fulda S (2003) Tumor resistance to apoptosis. Int J Cancer 124:511–515
3. Roos WP, Batista LFZ, Naumann SC et al (2007) Apoptosis in malignant glioma cells triggered by the temozolomide-induced DNA lesion O^6-methylguanine. Oncogene 26:186–197
4. Xu Y, Villalona-Calero MA (2002) Irinotecan: mechanisms of tumor resistance and novel strategies for modulating its activity. Ann Oncol 13:1841–1851
5. Jin Z, El Deiry WS (2005) Overview of cell death signaling pathway. Cancer Biol Ther 4:139–163

6. Kiechle FL, Zhang X (2002) Apoptosis: biochemical aspects and clinical implications. Clin Chim Acta 326:27–45
7. Rotonda J, Nicholson DW, Fazil KM et al (1996) The three-dimensional structure of apopain/CPP32, a key mediator of apoptosis. Nat Struct Biol 3:619–625
8. Grutter MG (2000) Caspases: key players in programmed cell death. Curr Opin Struct Biol 10:649–655
9. Lee BW, Olin MR, Johnson GL, Griffin RJ (2008) In vitro and in vivo apoptosis detection using membrane permeant fluorescent-labeled inhibitors of caspases. Methods Mol Biol 414:109–135
10. Kuzelová K, Grebenová D, Hrkal Z (2007) Labeling of apoptotic JURL-MK1 cells by fluorescent caspase-3 inhibitor FAM-DEVD-fmk occurs mainly at site(s) different from caspase-3 active site. Cytometry A 71:605–611
11. Barnett EM, Zhang X, Maxwell D et al (2009) Single-cell imaging of retinal ganglion cell apoptosis with a cell-penetrating, activatable peptide probe in an in vivo glaucoma model. PNAS 106:9391–9396
12. Ray P, De A, Patel M, Gambhir SS (2008) Monitoring caspase-3 activation with a multimodality imaging sensor in living subjects. Clin Cancer Res 14:5801–5809
13. Troy T, Jekic-McMullen D et al (2004) Quantitative comparison of the sensitivity of detection of fluorescent and bioluminescent reporters in animal models. Mol Imaging 3:9–29
14. Tuchin VV, Wang RK, Yeh AT (2008) Optical clearing of tissues and cells. J Biomed Opt 13:021101
15. Yang Y, Hong H, Zhang Y, Cai W (2009) Molecular imaging of proteases in cancer. Pubmed Central. http://www.ncbi.nlm.nih.gov/pmc/articles/PMC2838618/. Accessed in PMC 2010 March 15
16. Laxman B, Hall DE, Bhojani MS et al (2002) Noninvasive real-time imaging of apoptosis. PNAS 99:16551–16555
17. Liu JJ, Wang W, Dicker DT et al (2005) Bioluminescent imaging of TRAIL-induced apoptosis through detection of caspase activation following cleavage of Z-DEVD-aminoluciferin. Cancer Biol Ther 4:885–892
18. Kizaka-Kondoh S, Itasaka S et al (2009) Selective killing of hypoxia-inducible factor-1-active cells improves survival in a mouse model of invasive and metastatic pancreatic cancer. Clin Cancer Res 15:3433–3441
19. Hickson J, Ackler S, Klaubert D et al (2010) Noninvasive molecular imaging of apoptosis in vivo using a modified firefly luciferase substrate, Z-DEVD-aminoluciferin. Cell Death Differ 17:1003–1010
20. Zeng L, Kizaka-Kondoh S, Itasaka S et al (2007) Hypoxia inducible factor-1 influences sensitivity to paclitaxel of human lung cancer cell lines under normoxic conditions. Cancer Sci 98:1394–1401
21. Del Bene F, Germani M, De Nicolao G et al (2009) A model-based approach to the in vitro evaluation of anticancer activity. Cancer Chemother Pharmacol 63:827–836
22. Friedman HS, Kerby T, Calvert H (2000) Temozolomide and treatment of malignant glioma. Clin Cancer Res 6:2585–2597
23. Nair JS, de Stanchina E, Schwartz GK (2009) The topoisomerase I poison CPT-11 enhances the effect of the Aurora B kinase inhibitor AZD1152 both in vitro and in vivo. Clin Cancer Res 15:2022–2030
24. Shah K, Tung CH, Breakefield XO et al (2005) In vivo imaging of S-TRAIL-mediated tumor regression and apoptosis. Mol Ther 11:926–931
25. Lindner D, Raghavan D (2009) Intra-tumoural extra-cellular pH: a useful parameter of response to chemotherapy in syngeneic tumour. lines Br J Cancer 100:1287–1291
26. Tiefenthaler M, Amberger A, Bacher N et al (2001) Increased lactate production follows loss of mitochondrial membrane potential during apoptosis of human leukaemia cells. Br J Haematol 114:574–580

27. Tisi L et al. (2010). PH tolerant luciferase. US Patent 68,739. Washington, DC. US Patent and Trademark Office http://ip.com/patapp/US20100068739. 18 May 2010

28. Ekert PG, Silke J, Vaux DL (1999) Caspase inhibitors. Cell Death Differ 6:1081–1086

29. Darzynkiewicz Z, Bedner E, Smolewski P et al (2002) Detection of caspases activation in situ by fluorochrome-labeled inhibitors of caspases (FLICA). Meth Molec Biol 203:289–299

30. Tan DS, Thomas GV, Garrett MD et al (2009) Biomarker-driven early clinical trials in oncology: a paradigm shift in drug development. Cancer J 15:406–420

31. Hurko O (2009) The uses of biomarkers in drug development. Ann N Y Acad Sci 1180:1–10